Phys Chem Minerals (2001) 28: 177–187

ORIGINAL PAPER

A. Bosenick · M. T. Dove · V. Heine · C. A. Geiger

Scaling of thermodynamic mixing properties in garnet solid solutions

Received: 8 March 2000 / Accepted: 1 October 2000

Abstract The volumes and enthalpies of mixing, ΔV^{Mix} and ΔH^{Mix}, of binary solid-solution aluminosilicate garnets have been studied by computer simulation. The use of "average atoms" to simulate solid solution was found to give results that are considerably different from those obtained by calculating and averaging over many configurations of cations at a given composition. Although we expect mineral properties calculated from model calculations to be correct only on a qualitative rather than a quantitative scale, fair agreement with experiment was obtained where carefully tested potential parameters were used. The results show that mixing behaviour in these materials is controlled by local strain and relaxation effects resulting from the atomic size mismatch of the mixing divalent cations. In particular, ΔV^{Mix} and ΔH^{Mix} are shown to scale quadratically with the volume difference between the end members, and to vary essentially symmetrically with composition, with a moderate dependence on the degree and nature of cation order. We conclude that computer modelling should be useful in providing detailed qualitative information about the mixing properties of solid solutions, which can help to better constrain and interpret experimental results.

Key words Aluminosilicate garnets · Computer simulation · Solid solutions · Mixing properties

A. Bosenick · M. T. Dove (✉)
Department of Earth Sciences,
University of Cambridge,
Downing Street, Cambridge CB 23EQ, UK
e-mail: martin@esc.cam.ac.uk
Tel.: +44-1223-333482; Fax: +44-1223-333450

V. Heine
Cavendish Laboratory,
University of Cambridge,
Madingly Road, Cambridge CB3 OH2, UK

C. A. Geiger
Institut für Geowissenschaften der Christian-Albrechts-Universität zu Kiel, Olshausenstr. 40, 24098 Kiel, Germany

Introduction

Where a mineral assemblage preserved in a rock is recording a state of chemical equilibrium, thermodynamics can be used to unravel its P, T history. Such geothermobarometric calculations require an accurate knowledge of the physicochemical properties of the constituent minerals, including their pressure, temperature and compositional dependency. A knowledge of the variation of the thermodynamic properties with composition, i.e. of the thermodynamic mixing properties, is of particular significance because many pressure and temperature indicators are based on inter- or intracrystalline cation exchange reactions and, hence, involve one or more solid solution phases.

The determination of the thermodynamic mixing properties for rock-forming solid solutions is not only a costly and time-consuming task, but it is also hindered by various experimental difficulties. The derivation of mixing properties from phase equilibrium studies is frequently hampered by slow kinetics of the mineral reactions. Direct measurements of the enthalpies ΔH^{Mix} and volumes of mixing ΔV^{Mix}, by calorimetry and precise diffraction measurements of the lattice constants, respectively, require high-quality synthetic or natural samples. These may be difficult to obtain in sufficient amounts as single-phase material. In addition, minerals containing transition elements may suffer from non-stochiometry, or the samples may be chemically inhomogeneous. Finally, even for very pure and homogeneous samples, insufficient grain size may lead to problems in determining their exact composition by microprobe analysis. In any case, uncertainties in the chemical composition propagate into the measured thermophysical properties and thus lead to comparatively large uncertainties in the mixing properties.

As one of the most important rock-forming solid solutions, the aluminosilicate garnets $X_3Al_2Si_3O_{12}$, where X = Mg (pyrope, abbreviated Py), Fe^{2+} (almandine, Al), Mn^{2+} (spessartine, Sp), and Ca (grossular, Gr),

have been the subject of intensive studies of phase equilibrium, thermodynamic and crystal chemical properties. References to these works are given in Geiger (1999), Ganguly et al. (1996) and Mukhopadhyay et al. (1997). In principle, the combination of phase equilibrium studies and direct measurements of ΔH^{Mix} and ΔV^{Mix} using either least-squares regression methods (e.g. Holland and Powell 1985; Powell and Holland 1993) or mathematical programming (e.g. Berman et al. 1986; Olbricht et al. 1994) should lead to an internally consistent thermodynamic dataset. However, in spite of the diversity of available experimental data, their relatively large uncertainties result in a fair to poor agreement between different proposed models about the mixing properties of garnets (Geiger 1999). Hence, a better theoretical understanding of the thermodynamic mixing properties is needed to guide the interpolation and extrapolation from scanty experimental data.

The macroscopic thermodynamic properties of a phase are determined by its chemistry and structure. The effects of cation substitution on the properties of a solid solution mineral are a consequence of (1) size differences between the mixing cations, (2) differences in their bonding character and (3) different valence states. In isovalent solid solutions, where equally charged cations are mixed, as in the case of aluminosilicate garnets, only the first two factors have to be taken into account. Of these, the size difference between the cations being mixed is usually the most important. Already in 1974 Ganguly and Kennedy used, in addition to experimental data, cation size considerations to derive approximate mixing temperatures for three garnet binaries. Davies and Navrotsky (1983) studied size effects on mixing properties of various binary solid solutions, including oxide and alkali halide systems, and observed linear and quadratic correlations with the volume mismatch of the end-member phases. More recently, several authors noted that the deviations from ideal thermodynamic mixing in different aluminosilicate garnet binaries are larger for larger differences between the sizes of mixing cations (Geiger and Rossmann 1994; Ungaretti et al. 1995; Geiger and Feenstra 1997). In the case of the volumes of mixing, their deviations from ideality appear to be a function of the volume mismatch of end members (Geiger 1999, 2000). However, as illustrated in Fig. 1, it is uncertain whether ΔV^{Mix} varies linearly or quadratically with the volume difference ($V_{Large} - V_{Small}$) between two end members. There are only six binary mixtures between the four end members and the behaviour with $V_{Large} - V_{Small}$ cannot be inferred unambiguously from the six experimental points in Fig. 1.

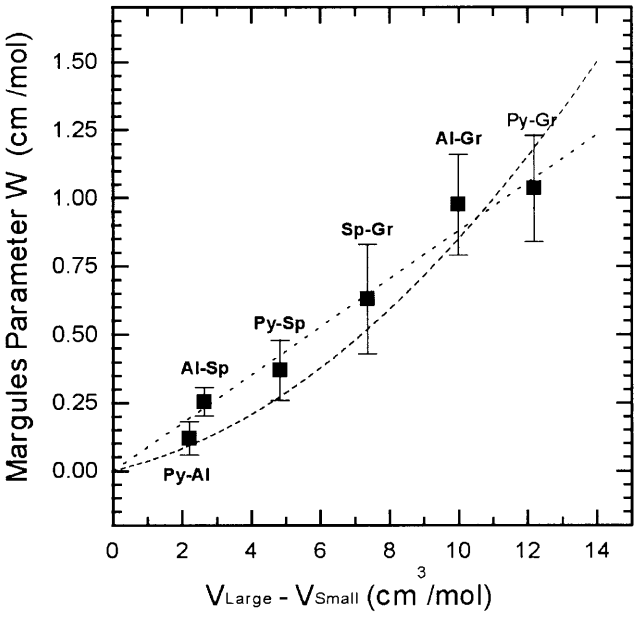

Fig. 1 Variation of the deviations from ideality for the volumes of mixing, quantified using the symmetric Margules parameter, W^V, plotted against the volume difference between the two corresponding end members. The sources for the different experimental data are summarised in Table 1. It is uncertain from these data whether W^V varies linearly (*dotted curve*) or quadratically (*dashed curve*) with $V_{Large} - V_{Small}$

Table 1 Experimental mixing properties of various garnet binary solid solutions. Values *in parentheses* represent uncertainties

Solid solution	$V_{Large} - V_{Small}$ ($cm^3\ mol^{-1}$)	Margules parameter W^V ($cm^3\ mol^{-1}$)	Source of experimental data
Py–Al	2.196	0.12 (6)	Geiger and Feenstra (1997)
Al–Sp	2.626	0.25 (5)	Geiger and Feenstra (1997)
Py–Sp	4.822	0.37 (11)	von Saldern (1994)
Sp–Gr	7.352	0.63 (20)	Rodehorst et al. (in prep.)
Al–Gr	9.978	0.97 (19)	Geiger et al. (1987)
Py–Gr	12.175	1.03 (20)	Ganguly et al. (1993), Bosenick and Geiger (1997)
		W^H_{cal} ($kJ\ mol^{-1}$)	
Py–Al	2.196	16.8 (6.1)	Geiger et al. (1987)
Al–Gr	9.978	−1.9 (5.9)	Geiger et al. (1987)
Py–Gr	12.175	37.1 (4.6)	Newton et al. (1977)
		W^H_{spec} ($kJ\ mol^{-1}$)	
Py–Al	2.196	0	Boffa Ballaran et al. (1999)
Al–Gr	9.978	20	Boffa Ballaran et al. (1999)
Py–Gr	12.175	33	Boffa Ballaran et al. (1999)

The aim of the present study is to use computer simulations to gain as much understanding as possible about the systematics of the thermodynamic mixing properties of aluminosilicate garnets. These properties are the excess volume ΔV^{Mix} and the excess enthalpy ΔH^{Mix}, which are defined precisely below. In particular, we want to determine the exact relationship between the volumes of mixing and the size difference between the cations being mixed.

Simulations of disordered solid solutions involve many calculations with randomised atomic arrangements on the cation sites in a supercell, and then averaging the results. It is beyond presently available computer power to do this with ab initio simulations, in which the Schrödinger equation is solved for all the valence electrons (within the pseudopotential approximation) to obtain chemical bonding and charge densities acurately (Payne et al. 1992). Instead, the interactions between atoms are represented by empirical interatomic potentials fitted to a wider range of data on minerals (Catlow and Mackrodt 1982a; Cormack 1999). Acknowledging that quantitative reliable data are best obtained by experimental studies in the laboratory, our aim is to study the effect of differing cation properties on the mixing properties of solid solutions rather than obtaining quantitative data. However, our results are in fair agreement with experiment, sufficiently good to give confidence in the microscopic picture they give. The random nature of the cation distribution in a disordered solid solution results in local strains and atomic relaxations due to differing cation sizes. These play the key role in determining the thermodynamic mixing properties. Besides the main issue of how $V_{\mathrm{Large}} - V_{\mathrm{Small}}$ affects ΔV^{Mix} (and ΔH^{Mix}), the simulations give information on the effect of bonding character, on the coupling of mixing properties to cation order, and on how symmetrical the mixing behaviour is with respect to composition. Before showing and discussing these results, we will first, in the following section, briefly review the properties of binary solid solutions and define the terminology used in the present paper. Then we will describe the simulation methods used. In particular, we will discuss (1) two phenomenologically different approaches to simulate solid solution minerals and (2) the approach of mixing artificial cations, which allows us to study the effect of varying cation size differences on the mixing properties independently of any other influences.

Terminology and mixing properties

The thermodynamic formalism used in the Earth Sciences community to describe the mixing properties of solid solutions has been summarised in various reviews and textbooks (e.g. Thompson 1969; Ganguly and Saxena 1987; Chatterjee 1991; Cemič 1988; Navrotsky 1987).

In solid solutions two or more different cations share a common crystallographic site. Let (A, B)Z be a binary solid solution in which the two cations A and B mix on the crystallographic site X. The fraction of cation A on site X is x_{A} and that of cation B is $x_{\mathrm{B}} = (1 - x_{\mathrm{A}})$. Let Z represent the rest of the crystal structure that is not directly involved in the mixing process, which is therefore the same for all solid solution compositions and the two end members AZ and BZ.

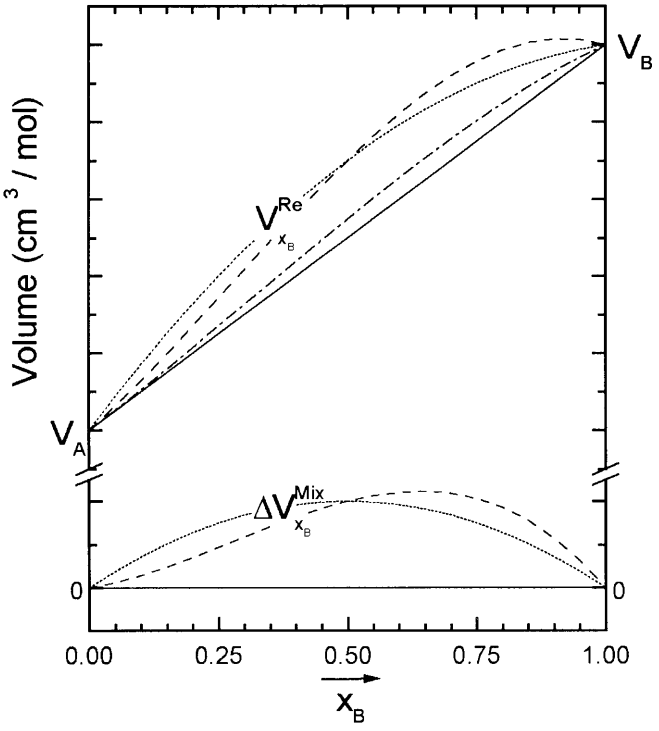

Fig. 2 General behaviour of the volumes (*upper part*) and volumes of mixing (*lower part*) for a binary solid solution. The *straight lines* show the ideal thermodynamic, i.e. linear, mixing behaviour resulting in zero ΔV^{Mix} across the binary. The *dotted line* shows positive symmetric deviations from ideal mixing and the *dashed line* shows a positive asymmetric deviation from ideal mixing. The plotted deviations are highly overestimated for the sake of clarity: in reality, deviations from ideality are much smaller as shown by the *dash-dotted line* for the system pyrope–grossular

According to the thermodynamic definition, the volume of a solid solution composition is ideal, if it is identically equal to the volume of a mechanical mixture of the same composition, i.e. if it is a linear combination of the stochiometric sum of the volumes of the end-member components:

$$V^{\mathrm{Ideal}} = x_{\mathrm{A}} V_{\mathrm{A}} + x_{\mathrm{B}} V_{\mathrm{B}} = V_{\mathrm{A}} + x_{\mathrm{B}}(V_{\mathrm{B}} - V_{\mathrm{A}}) \ . \qquad (1)$$

The volumes of mixing are given by the difference between the real, observed volumes of the solid solution compositions and their values in the case of ideal mixing. They are also referred to as excess volumes of mixing:

$$\Delta V^{\mathrm{Mix}} = \Delta V^{\mathrm{Ex}} = V^{\mathrm{Real}} - V^{\mathrm{Ideal}} \ . \qquad (2)$$

Figure 2 shows a sketch of the possible behaviour of the volumes and the excess volumes of mixing in a binary solid solution. The compositional dependence of the mixing properties of solid solutions is approximated by empirical polynomials. Usually, either of two functions

can be used; first, symmetric deviations from ideal mixing can be described by a Margules function with one fitting parameter, W^V:

$$\Delta V^{\mathrm{Mix}} = (1 - x_{\mathrm{B}}) x_{\mathrm{B}} W^V \quad . \tag{3}$$

Second, asymmetric deviations from ideal mixing can be approximated by a Margules polynomial with two parameters, W^V_{AB} and W^V_{AB}, of the form:

$$\Delta V^{\mathrm{Mix}} = (1 - x_{\mathrm{B}})^2 x_{\mathrm{B}} W^V_{\mathrm{BA}} + (1 - x_{\mathrm{B}}) x^2_{\mathrm{B}} W^V_{\mathrm{AB}} \quad . \tag{4}$$

The enthalpies of mixing behave in a way similar to the volumes of mixing, so that the above formalism can be applied accordingly.

Method of simulation

Parameterised model calculations

For the present study, we have undertaken static lattice energy calculations based on transferable empirical potential models using the program GULP (Gale 1997). The basic principles of lattice energy calculations are well documented (e.g. Burnham 1985; Price et al. 1987; Catlow 1988; Dove 1993). In short, the interactions between the atoms are described by potential functions, Φ_k, which contain empirical parameters. The sum over all the interatomic potential functions, Φ_k, gives the lattice energy of a crystal:

$$E = \sum_k \Phi_k \quad . \tag{5}$$

The crystal structure is at equilibrium when the lattice energy is at a minimum value with respect to all structural parameters $\{p_l\}$:

$$\frac{\partial E}{\partial p_l} = 0 \quad \text{for all } l \quad . \tag{6}$$

Hence, the equilibrium structure can be obtained by adjusting the lattice parameters and the positions of all atoms until the lattice energy has reached its minimum. This procedure has neglected the effects of temperature through the lattice dynamics, but for the present work this is not a significant point.

For our calculations, we have used a set of potential functions known as the THB model. This model was initially developed for quartz (Sanders et al. 1984), but has been found to work well for silicate minerals in general (e.g. Dove 1989; Winkler et al. 1991; Patel et al. 1991). In the THB model, pair interactions between two neighbouring atoms, i and j, are modelled as a sum of long-range Coulomb interactions, short-range repulsive interactions and dispersive interactions for polarisable ions:

$$\varphi_{ij}(r_{ij}) = \frac{Q_i Q_j}{4\pi\varepsilon_0 r_{ij}} + B_{ij} \exp\left(-\frac{r_{ij}}{\rho_{ij}}\right) - \frac{A_{ij}}{r^6_{ij}} \quad . \tag{7}$$

The first term in the pair-potential function is the Coulomb energy: Q_i and Q_j are the charges on the ions, ε_0 is the permittivity of free space and r_{ij} is the interionic distance. The second term is the Born–Mayer repulsive energy potential. The third term in Eq. (7) describes the dispersive interaction. Together, the last two terms are generally referred to as the Buckingham pair potential. The parameters B_{ij}, ρ_{ij} and A_{ij} are empirical constants, which depend on the atom pair. The cations are represented as rigid ions and formal charges are assumed for their Coulomb interactions. To account for their polarisability, the oxygen atoms are modelled using a core-shell model, i.e. a combination of a massless charged shell and a central core that carries all the ionic mass and the residual ionic charge. The core and the shell interact by a harmonic interaction of the form:

$$\varphi(d) = \frac{1}{2} K d^2 \quad , \tag{8}$$

where d is the separation between the centres of core and shell and K is an empirical force constant for the interaction. An important interaction that is incorporated in the THB model is a bond-bending potential which accounts for a certain degree of covalent bonding, in so far as it keeps the bond angles of coordination polyhedra near some ideal value:

$$\varphi(\theta) = \frac{1}{2} k (\theta - \theta_0)^2 \quad , \tag{9}$$

where k is an empirical force constant, θ is the polyhedral angle and θ_0 is the respective angle of the undistorted polyhedron with values 109.47° for SiO_4 tetrahedra and 90° for AlO_6 octahedra. The complete set of empirical parameters used for the present calculations is given in Table 2. These potentials have been thoroughly tested for their ability to model the structural and physical prop-

Table 2 Empirical potential parameters

Buckingham pair potential between cation cores and O shells				
	B [eV]	ρ [Å]	A [eV/Å^6]	Reference[a]
$Si^{4+} \cdots O^{-2.8482}_{\mathrm{shell}}$	1283.9073	0.3205	10.662	(1)
$Al^{3+} \cdots O^{-2.8482}_{\mathrm{shell}}$	1460.3	0.2991		(2)
$O^{-2.8482}_{\mathrm{shell}} \cdots O^{-2.8482}_{\mathrm{shell}}$	22 764.0	0.1490	27.880	(1)
$Mg^{2+} \cdots O^{-2.8482}_{\mathrm{shell}}$	1428.50	0.2945		(3)
$Ca^{2+} \cdots O^{-2.8482}_{\mathrm{shell}}$	2272.70	0.2986		(4)
$Fe^{2+} \cdots O^{-2.8482}_{\mathrm{shell}}$	694.10	0.3399		(5)
Core-shell interaction between O core and O shell				
	K [eV Å^{-2}]			
$O^{+0.8482}_{\mathrm{Core}} \cdots O^{-2.8482}_{\mathrm{Shell}}$	74.9200			(1)
Bond-bending interactions				
	k [eV rad^{-2}]	θ_0[°]		
O^{2-}–Si^{4+}–O^{2-}	2.09724	109.47		(1)
O^{2-}–Al^{3+}–O^{2-}	2.09724	90.0		(1)

[a] (*1*) Saunders et al. (1984); (*2*) Catlow et al. (1982), (*3*) Price et al. (1987); (*4*) Bush et al. (1994); (*5*) Lewis (1984)

erties of both pyrope and grossular garnets (for grossular it was found necessary to choose a different model for the Ca–O potential than that used by Winkler et al. 1991). Albeit not perfect, the model was found to have sufficient predictive power to model structural details such as the distortion of the SiO_4-tetrahedra and AlO_6-octahedra in garnets as well as to predict physical properties such as the IR frequencies to better than 10%. Details of the tests of the model for the pyrope-grossular series, and comparisons with different parameterisations, are given by Bosenick et al. (2000). The Fe–O potential has not been tested to the same level, and we will therefore refrain from any attempt to deduce quantitative predictions from simulations undertaken with this potential. We will use it merely to demonstrate the effect of different bonding characters on the mixing properties, and to show that these effects are eliminated within any solid-solution series.

Simulation of solid solutions

Mixing potentials

The simulation of a binary solid solution can be done using two different phenomenological approaches which can be regarded as two different levels of approximation. Firstly, we can use a mean-field or virtual crystal model and use an effective average potential for the X-site to describe an occupancy, x_B, of one end-member cation and $(1-x_B)$ of the other end-member cation. This approach requires the mixing of the pair potentials φ_{A-j} and φ_{B-j} of the two cations *A* and *B*. Winkler et al. (1991) proposed a simple mixing scheme using the condition that the first and second derivatives of the effective potential, $\varphi_{\text{eff}-j}$, should be equal to the stoichiometric sum of the derivatives of the potentials of the constituent cations at the average atomic distance r_0:

$$\left(\frac{\partial\varphi_{\text{eff}-j}}{\partial r}\right)_{r=r_0} = (1-x_B)\left(\frac{\partial\varphi_{A-j}}{\partial r}\right)_{r=r_0} + x_B\left(\frac{\partial\varphi_{B-j}}{\partial r}\right)_{r=r_0}, \quad (10a)$$

$$\left(\frac{\partial^2\varphi_{\text{eff}-j}}{\partial r^2}\right)_{r=r_0} = x_B\left(\frac{\partial^2\varphi_{A-j}}{\partial r^2}\right)_{r=r_0} + (1-x_B)\left(\frac{\partial^2\varphi_{B-j}}{\partial r^2}\right)_{r=r_0}. \quad (10b)$$

The values for $\rho_{\text{eff}-j}$ and $B_{\text{eff}-j}$ are then given by:

$$\rho_{\text{eff}-j} = \frac{(1-x_B)\rho_{A-j}^{-1}B_{A-j}\exp\left(-\frac{r_0}{\rho_{A-j}}\right) + x_B\rho_{B-j}^{-1}B_{B-j}\exp\left(-\frac{r_0}{\rho_{B-j}}\right)}{(1-x_B)\rho_{A-j}^{-2}B_{A-j}\exp\left(-\frac{r_0}{\rho_{A-j}}\right) + x_B\rho_{B-j}^{-2}B_{B-j}\exp\left(-\frac{r_0}{\rho_{B-j}}\right)} \quad (11a)$$

$$B_{\text{eff}-j} = \frac{(1-x_B)\rho_{A-j}^{-1}B_{A-j}\exp\left(-\frac{r_0}{\rho_{A-j}}\right) + x_B\rho_{B-j}^{-1}B_{B-j}\exp\left(-\frac{r_0}{\rho_{B-j}}\right)}{\rho_{\text{eff}-j}^{-1}\exp\left(-\frac{r_0}{\rho_{\text{eff}-j}}\right)}. \quad (11b)$$

The effective charge Q_{eff} is simply given by the weighted charge average of the atoms being mixed:

$$Q_{\text{eff}} = (1-x_B)Q_A + x_BQ_B. \quad (12)$$

r_0 was taken as a constant value of 2.35 Å, i.e. an average of the X–O bond lengths in the pyrope–grossular solid solution. Varying r_0 in a range equivalent to the variation in the X–O bond lengths between pyrope and grossular, i.e. 2.27 to 2.40 Å, has very little influence on the outcome of the simulations (Chall et al. unpubl. data).

By mixing potentials, one can create an average or virtual cation with properties such as its atomic size, valence and bonding character that are a weighted average of the properties of the two cations being mixed. Using average potentials for simulating a solid solution means that all X-sites are occupied by the same cation. As a result, all X-sites have exactly the same environment and no local relaxations or distortions occur. In other words, a binary (A, B)Z solid solution with complete cation disorder is approximated as a perfect crystal, called a virtual crystal of average atoms. This approach has been used in a number of studies, mainly to model complete disordered site occupancy of Al^{3+} and Si^{4+} in aluminosilicates (Winkler et al. 1991; Dove et al. 1993; Dove and Redfern 1997; Redfern et al. 1997. It was also used to simulate the mixing of Ca^{2+} and Mg^{2+} in the pyrope–grossular garnet solid solution by Winkler et al. 1991, but there is an error in part of the analysis given in that paper. Moreover, these authors used a different Ca–O pair potential to that used in the present study.). We also tested a site occupancy approach to define the virtual crystal. For the case of pyrope50grossular50, we placed half an Mg and half a Ca atom at each X-cation position. This is equivalent to using a simple average of Mg–O and Ca–O potentials. The results in this case agreed to 5 significant figures with the mixing formula (Eqs. 10 and 11) for the total volume and enthalpy, which supports the general robustness of our virtual crystal results.

Mixing cations in a supercell

The second more realistic approach to simulate solid solutions uses a supercell which is an $n \times n \times n$ enlarged unit cell containing N symmetrically equivalent X-sites. To simulate a solid solution with composition x_B, $n_A = (1-x_B) \times N$ cations of type A and $n_B = x_B \times N$ cations of type B are distributed over these X-sites. In relaxing such an arrangement, we switch off all symmetry constraints. Many different arrangements are possible, corresponding to various degrees and types of local order. When the supercell is repeated periodically, these arrangements become, in principle, distinct long-range ordering states of the original crystal. To study the properties of a random solid solution, one has to build up a database of many different arrangements of the cations and average

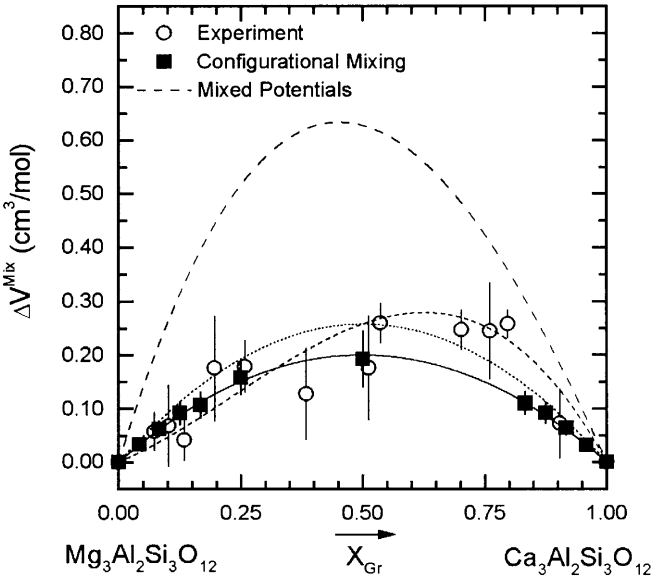

Fig. 3 Comparison of experimental and simulated volumes of mixing for the pyrope–grossular garnet binary. The experimental data (*open circles*) are taken from the most recent studies by Ganguly et al. (1993) and Bosenick and Geiger (1997). The *short dashed curve* shows an asymmetric fit to the experimental data and the *dotted line* a symmetric fit. The simulation using mixed potentials (*dashed curve*) give values that are larger by a factor of 2 to 3 than experiment. The results of simulations done by mixing cations in a supercell are shown as *full squares*. The corresponding *error bars* indicate the maximum scatter of the results due to different ordering states, i.e. different cation arrangements in the supercell. The *full line* through the latter results highlights their essentially symmetric deviation from ideal mixing

over their properties. Contrary to the approach of mixing potentials, each X-site is now occupied either by an A or B cation and this allows *local* structural relaxation to occur. The main limitation of the supercell approach is that it is much more computationally demanding than the method of averaging potentials.

The simulations of binary aluminosilicate garnets were done in a $1 \times 1 \times 1$ supercell, which contains 24 X-sites. Simulations were done for the following compositions: $n_A = 0$ (1), 1 (1), 2 (7), 3 (25), 4 (20), 6 (50), 12 (60), 18 (50), 20 (20), 21 (25), 22 (7), 23 (1), 24 (1), where the numbers in brackets indicate the total number of different arrangements calculated. Many more arrangements are possible for intermediate compositions: in the worst case there are $24!/(12!)^2$ possible arrangements, although symmetry (including translational symmetry) will reduce the total number of *independent* arrangement. We consider that we are using an acceptable sampling for reliable statistical analysis, given that the standard deviation on a mean value is independent of the sampling fraction. For every configuration the positions of all "atoms" (core and shell) and the size of the unit cell were allowed to relax, and there were no symmetry constraints on the positions of the atoms. However, the shape of the supercell was constrained to remain cubic, as it would be on average in a disordered garnet solid solution. It was previously shown that this constraint has a negligible effect on the results (Bosenick et al. 2000, and independent tests on other systems).

The main purpose of the present work is to study the effect of ionic size on the thermodynamic properties of the solid solutions. Clearly, the method of average atoms already models some properties, such as giving an excess volume across the solid solution as sketched in Fig. 3, but by comparing results from the two methods we can determine the influence of the local strains around various local ionic configurations in a disordered solid solution.

Extending the periodic table

In studying the role of ionic size, we are hampered by the paucity of data. In our solid solution garnets, we have only four divalent cations (Mg^{2+}, Fe^{2+}, Mn^{2+} and Ca^{2+}), of which two are transition elements that may introduce a significant degree of *d*-bonding. Clearly, systematic experimental studies could only be possible if the periodic table contained thousands of elements! One could then select a range of elements differing only in ionic radius but otherwise the same, and observe the trends. One of the advantages of computer simulation is that one can indeed create such a situation, by inventing new sets of interatomic potentials (Eqs. 7 to 9) to represent new cations. In our case, these cations will always have an ionic charge of +2 and will interact only with neighbouring oxygen atoms.

Unfortunately, this is not as straightforward as one might think. One tends to think about the ionic size as a constant value depending only on the coordination of the ion. However, ionic size is not a defined quantity: it is a simplified picture of ions neglecting their characteristic bonding behaviour in a distinct environment and the corresponding charge density distribution. In our parameterised model calculations, the cations are also not simply defined in terms of their size and charge: they are defined in terms of their interaction with neighbouring oxygen anions. In principle, the empirical parameter ρ_{ij} in the Buckingham potential (Eq. 7) defines the relative sizes of the atoms i and j because it is related to the equilibrium distance between them. The parameter B_{ij} is a measure of the hardness of the interaction (Dove 1993) and is related to the bonding character of the cation. However, B_{ij} and ρ_{ij} are highly correlated and should therefore not be varied separately. To obtain a sensible potential, we select two "real" elements A, B, and use the

Table 3 Definition of Eka-cations and lattice constants of corresponding Eka-end-member garnet

Label for Eka-cation	Fraction of potentials being mixed		Potential parameter between cation core–oxygen shell		Lattice constant of Eka-garnet (Å)
	$X_{Small–O}$	$X_{Large–O}$	B (eV)	ρ (Å)	
Mg	1.0	0.0	1428.50	0.2945	11.3225
Eka(75Mg/25Ca)	0.75	0.25	1637.79	0.2960	11.4440
Eka(50Mg/50Ca)	0.5	0.5	1848.60	0.2971	11.5498
Eka(25Mg/75Ca)	0.25	0.75	2060.36	0.2979	11.6429
Ca	0.0	1.0	2272.74	0.2986	11.7289
Eka(−25Mg/125Ca)	−0.25	1.25	2485.56	0.2991	11.8038
Eka(−100Mg/200Ca)	−1.0	2.0	3125.64	0.3003	12.0005
Fe	1.0	0.0	694.10	0.3399	11.4730
Eka(−100Mg/200Fe)	−1.0	2.0	439.08	0.3805	11.6319
Eka(−100Fe/200Ca)	−1.0	2.0	4638.79	0.2803	11.9020

Table 4 Definition and mixing properties of simulated solid solutions

Small end-member cation	Large end-member cation	ΔV_{AB} ($cm^3\ mol^{-1}$)	W^V ($cm^3\ mol^{-1}$)	W^H ($kJ\ mol^{-1}$)
Eka(Mg/Ca) solid solutions				
Mg	Eka(75Mg/25Ca)	3.553	0.083 (1)	6.0 (1)
Eka(50Mg/50Ca)	Ca	5.446	0.147 (2)	13.3 (1)
Mg	Eka(50Mg/50Ca)	6.711	0.279 (3)	21.0 (3)
Mg	Eka(25Mg/75Ca)	9.538	0.537 (7)	41.8 (6)
Eka(75Mg/25Ca)	Eka(−25Mg/125Ca)	10.979	0.612 (8)	53.7 (8)
Mg	Ca	12.192	0.811 (11)	59.9 (21)
Mg	Eka(−100Mg/200Ca)	20.828	2.168 (28)	185.2 (44)
Eka(Mg/Fe) solid solutions				
Mg	Fe	4.379	−0.088 (2)	
Mg	Eka(−100Mg/200Fe)	9.207	−0.235 (5)	
Eka(Fe/Ca) solid solutions				
Fe	Ca	7.777	0.589 (7)	
Fe	Eka(−100Fe/200Ca)	13.238	1.509 (11)	

same mixing formulae (Eqs. 10 and 11) with a chosen x_B to define an element of intermediate character. We can also choose values of x_B less than zero or greater than unity in order to extrapolate, i.e. to give a cation more extreme than A or B. We call these artifical elements Eka-cations, designated Eka(n_A.A/ · n_B · B) with $n_i = 100 \cdot x_i$ (from the prefix eka denoting in the same series, as used by Mendeleyev for predicting elements, such as eka-silicon, which is now germanium). By generating a sequence of Eka-cations based on the same two real elements, we create a series of different-sized cations, albeit with a minimal change in their bonding character.

We created three different series of Eka-cations: (1) Eka(n_{Mg}Mg/n_{Ca}Ca)-cations, that are a mixture of different amounts of the Mg–O and Ca–O potentials, (2) Eka(n_{Mg}Mg/n_{Fe}Fe)-cations, that are mixtures of Mg–O and Fe–O and (3) Eka(n_{Fe}Fe/n_{Ca}Ca)-cations, that are mixtures of Fe–O with the Ca–O potential (Table 3). These Eka-cations are then used as new elements in the supercell method to model different solid solutions. However, we modelled only solid solutions between Eka-cations of the same series. Accordingly, we have three different sets of solid solutions: Eka(Ca/Mg)-solid solutions, Eka(Mg/Fe)-solid solutions and Eka(Fe/Ca)-solid solutions. All solid solutions that are a mixture of two Eka(n_AA/n_BB)-cations are referred to as Eka(A/B)-solid solution series. The different Eka-cations and the mixtures calculated with them are given in Tables 3 and 4. By modelling solid solutions between Eka-cations of the same series, differences in bonding character between the mixing cations are minimised. Correspondingly, changes in the mixing properties within a series of solid solutions are directly related to the size difference of the cations being mixed. However, differences in bonding character are considerable between the three solid solutions series. We used the same sampling procedures for the same range of compositions as for our simulations of the pyrope–grossular series discussed earlier.

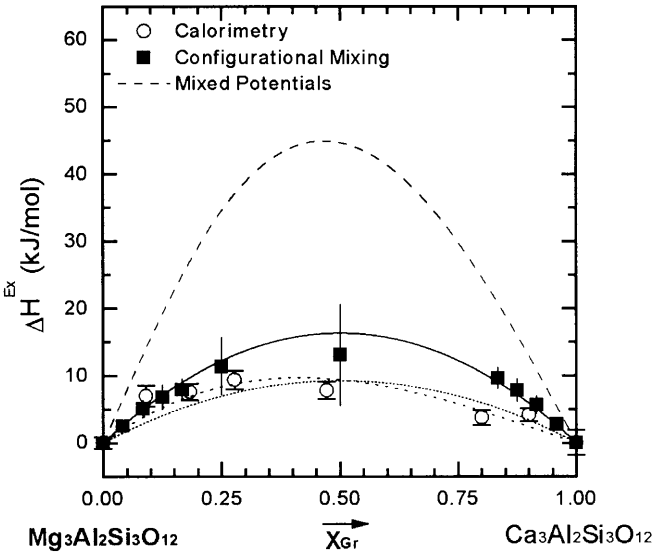

Fig. 4 Comparison of experimental and simulated enthalpies of mixing for the pyrope–grossular garnet binary. The experimental data (*open circles*) are taken from Newton et al. (1977). The *short dashed curve* shows an asymmetric fit to the experimental data and the *dotted line* a symmetric fit. The simulation using mixed potentials (*dashed curve*) give values that are larger by a factor of more than 5 than the experimental data. The results of simulations done by mixing cations in a supercell are shown as *full squares*. The corresponding *error bars* indicate the maximum scatter of the results due to different ordering states. The *full line* through the latter data highlights their essentially symmetric deviation from ideal mixing

Results

Comparison of simulation methods for the pyrope–grossular solid solution

To compare the two different levels of approximating solid solutions, we modelled pyrope–grossular garnets using both the approach of mixing potentials and that of mixing the cations Ca^{2+} and Mg^{2+} in a supercell. The results for the volumes of mixing are shown in Fig. 3, together with the most recent experimental data from Ganguly et al. (1993) and Bosenick and Geiger (1997). A similar comparison between experimental and simulated data was made for the enthalpies of mixing (Fig. 4). Although it should be kept in mind that parameterised model calculations are not likely to get the energies right on a quantitative scale (e.g. Dove et al. 2000), enthalpies of mixing are related to energy differences, which are more likely to be correct. The experimental data plotted in Fig. 4 are enthalpies of mixing obtained by solution calorimetric measurements, as quoted by Newton et al. (1977).

Simulations with mixed potentials result in volumes and enthalpies of mixing that are by several factors larger than those obtained with the supercell approach. A similar qualitative effect on ΔV^{Mix} was previously noted by Chall et al. (unpubl. data), who used a different Ca–O potential to simulate pyrope–grossular garnets using both simulation methods, and also by Purton et al. (1998) in work on binary oxides. Our simulations with the supercell method are in good enough quantitative agreement with the experimental data to give us confidence in the microscopic picture they give. Clearly, the better approach to model garnet solid solutions is that of mixing cations in a supercell. From a structural point of view, the main difference between the two different methods of approximation is that in the virtual crystal, all X-sites, and hence their environments, are exactly equivalent, while in the supercell approach each X-site is occupied by either of two cations, and local relaxations are allowed to occur. The large discrepancy in ΔV^{Mix} and ΔH^{Mix} obtained with the two different simulation methods shows the significant influence that local structural relaxations have on the macroscopic thermodynamic properties of garnet solid solutions. Because of the absence of rigid unit modes in the garnet structure (Hammonds et al. 1998), which would have allowed the SiO_4-tetrahedra and AlO_6-octahedra that form the corner-sharing three-dimensional garnet framework to rotate without being distorted, these local distortions will involve a combination of local rotation of the framework polyhedra and a distortion from their average shape (Bosenick et al. 2000). Simulating solid solutions by mixing potentials does not allow for local relaxations. To simulate such structural mechanism the supercell method has to be applied.

There has been some discussion in the literature concerning the asymmetry in the mixing properties of pyrope–grossular garnet solid solutions (e.g. Geiger

1998). Older measurements of the volumes of mixing of pyrope–grossular garnets show such a large scatter that one has to assume symmetric mixing (Berman 1980). However, more recent measurements by Ganguly et al. (1993) and Bosenick and Geiger (1997) suggest an asymmetric behaviour in ΔV^{Mix}. In the case of the enthalpies of mixing the form of the asymmetry is questionable. The calorimetric measurements show asymmetric behaviour with the largest deviations in pyrope-rich garnets (Newton et al. 1977), although the errors that propagate through the analysis give some uncertainty on this result. Calculations based on an elastic model suggest an opposed asymmetry (Ganguly et al. 1993). The simulations with both methods presented here give mixing volumes and enthalpies of mixing that are essentially symmetric with composition and therefore do not further constrain the asymmetry of mixing properties. However, since our model properly incorporates strain effects, the experimentally observed asymmetry must be related to sources other than simply strain. Differences in bonding character, as proposed by Ungaretti et al. (1995) and Quartieri et al. (1995), are the only likely source.

That pyrope–grossular solid solutions have a certain degree of short-range order, but no long-range order has been shown by ^{29}Si MAS NMR spectroscopy (Bosenick et al. 1995, 1999) and Monte Carlo simulations (Bosenick et al. 2000). It is of great interest whether different degrees of order have a measurable influence on the enthalpies and volumes of garnet solid solutions. If they do, the great scatter in the different datasets for the volumes of mixing could be related to different ordering states. Simulations by mixing cations in a supercell have been done on many differently ordered arrangements of Ca and Mg on the X-sites and the volumes and enthalpies of mixing were found to be slightly dependent on the ordering state. Because the supercell simulations and experiments are in fair quantitative agreement, the coupling of the volumes or ΔV^{Mix} with the ordering state deduced from the simulations is likely to be of the right order of magnitude. The absolute observed scatter in the lattice constants is about 0.002 Å, which corresponds to a scatter in the garnet molar volumes of 0.05 $\mathrm{cm^3/mol^{-1}}$. Precise X-ray diffraction measurements allow the determination of lattice constants with uncertainties below 0.001 Å. In principle, variations in the volumes related to different ordering states should therefore be measurable. However, to observe this experimentally would require a series of differently ordered samples that have exactly the same composition, because any uncertainty in the composition would propagate into the volume uncertainty and swamp possible ordering contributions. In spite of very small uncertainties in the composition of their synthetic pyrope–grossular garnets, Bosenick et al. (1999) observed a slight dependence of the lattice constants on the garnet syntheses temperatures. Considering the present simulations, these may well be related to differences in the ordering state. The observed variation of the mixing properties with the ordering state is shown in Figs. 3 and 4 in the form of error bars, which give the absolute observed scatter, i.e. the minimum and maximum observed values. The largest variations with the ordering state in ΔV^{Mix} and ΔH^{Mix} are observed for the intermediate composition $x_{\mathrm{Ca}} = 0.5$. In the case of the volumes of mixing, these variations are of the same order of magnitude as the experimental uncertainties of the volumes of mixing, if the errors in composition are taken into account. However, because the dependency of the lattice constants, and hence of ΔV^{Mix}, on the ordering state is relatively small, most of the scatter between different experimental datasets is likely to result from uncertainties in the garnet compositions rather than differing ordering states.

Quadratic scaling of mixing properties

The effect of ionic size on the thermodynamic mixing properties of binary garnets was studied with three different series of solid solutions: Eka(Ca/Mg)-, Eka(Mg, Fe)- and Eka(Fe, Ca)-solid solutions (Table 4). As discussed above, within each of the solid solution series it is only the size of the cations that is changing, while differing bonding characters have practically been eliminated. However, differences in the bonding character exist between the different solid solution series.

The influence of the size difference of the mixing cations can be parameterised in different ways (Davies and Navrotsky 1983). As the assignment of cation radii is always somewhat arbitrary, we decided to analyse the magnitude of ΔV^{Mix} and ΔH^{Mix} in terms of the volume mismatch between the two end members of the solid solutions, i.e. $|V_{\mathrm{A}} - V_{\mathrm{B}}| = \Delta V_{\mathrm{AB}}$, i.e. the difference between the volume of the larger and the smaller end-member ($V_{\mathrm{Large}} - V_{\mathrm{Small}}$).

As a measure for the magnitude of the deviation from ideal mixing, we chose the symmetric Margules parameters W^V and W^H (Eq. 3). These parameters are summarised in Table 4 for the different solid solutions that were simulated by mixing different Eka-cations. Symmetric Margules parameter were also fitted to the experimental data available and the results are summarised in Table 1. Some of the experimental data sets show some degree of asymmetry with respect to composition. However, the largest asymmetry is present along the pyrope–grossular binary. Although in this case a two-parameter Margules fit describes the experimentally observed behaviour across the binary better than a one-parameter symmetric fit, the latter gives us an averaged value of the absolute magnitude of the deviation from ideal mixing. Indeed, a symmetric fit is a special case of the asymmetric fit with $W_{\mathrm{sym}} = W_{\mathrm{AB}} = W_{\mathrm{BA}}$. Hence, using a symmetric fit to describe the average deviations from ideal mixing is equivalent to averaging the Margules parameters, W_{AB} and W_{BA}, of an asymmetric fit to the data.

The dependence of the magnitude of the volumes of mixing on ΔV_{AB}, i.e. the variation of W^V with the volume mismatch, is shown in Fig. 5 for the three different

series of solid solution. The most expanded solid solution series studied is that of Eka(Ca/Mg)-solid solutions. These include solid solutions between a "real parent element" Mg or Ca and an Eka(n_{Mg}Mg/n_{Ca}Ca)-cation, as well as solid solutions between two different Eka(n_{Mg}Mg/n_{Ca}Ca)-cations. The symmetric Margules parameters of this series of Eka(Ca/Mg)-solid solutions shows unambiguously a quadratic correlation with the volume mismatch between the end members:

$$W^V \propto \Delta V_{AB}^2 \ . \tag{13}$$

For the two other series, we modelled in each case only two different solid solutions, because it became immediately clear that for both series W^V also scales quadratically with the volume mismatch, albeit with different coefficients. The solid solution series created from Eka(n_{Mg}Mg/n_{Ca}Ca)-cations shows a positive scaling of W^V with ΔV_{MgCa}^2, the series created from Eka(n_{Fe}Fe/n_{Ca}Ca)-cations has a stronger positive dependence, and those created from Eka(n_{Fe}Fe/n_{Ca}Ca)-cations show a slightly negative correlation of W^V with ΔV_{MgFe}^2. It should be noted here that strict compliance with Vegard's rule, i.e. a linear change in the lattice constants with composition, would, in fact, give a slightly negative volume of mixing and hence a decrease of W^V with ΔV_{AB}^2, because volume is the cube of the lattice constant. However, a linear mixing of lattice constants would give a more negative value of $W^V/\Delta V_{AB}^2$ than that observed for the Eka(Mg/Fe)-solid solutions, indicating that this series, like the other two solid-solution series, possesses a positive deviation from Vegard's law, albeit a very small one. There exists no overt correlation between the different solid solution series.

Hence, in our simulations differences in bonding character between the mixing cations have profound effects on the mixing properties of garnet solid solutions which show no correlation with ΔV_{AB}. From the observation that the Margules parameter of all three solid-solution series correlates in the same manner with ΔV_{AB} it can be concluded that differences in cation size of the mixing cations result in quadratic dependence of W^V on the volume mismatch between the end members. As a result, the experimentally determined Margules parameter in Fig. 1 should be approximated with a quadratic rather than a linear function of ΔV_{AB} if the changes were solely due to varying cation size differences. That the experimentally observed relationship between W^V and ΔV_{AB} is indeed well modelled by a quadratic function, suggests, in turn, that for garnet solid solutions the volumes of mixing are mainly controlled by the size differences of the X-site cations and that other effects, such as bonding character, are only of secondary importance.

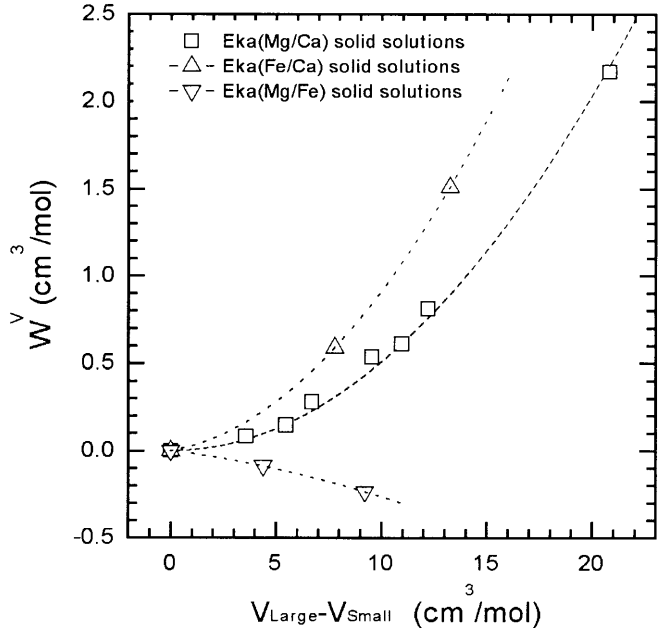

Fig. 5 Simulated deviations from ideality for the volumes of mixing, quantified as W^V, for three different series of solid solutions. Within every series, differences in mixing properties between different solid solution are only due to differing cation size differences, while between the series changes in bonding characteristics also occur. For every individual series a quadratic scaling of W^V with the volume mismatch between the end members, $V_{Large} - V_{Small}$, is observed, while no clear correlation exists between the different solid-solution series. Hence, differences in cation size of the mixing cations result in non-idealities in the volumes of mixing that increase quadratically with the volume difference between the end members, i.e. $W^V \propto \Delta V_{AB}^2$

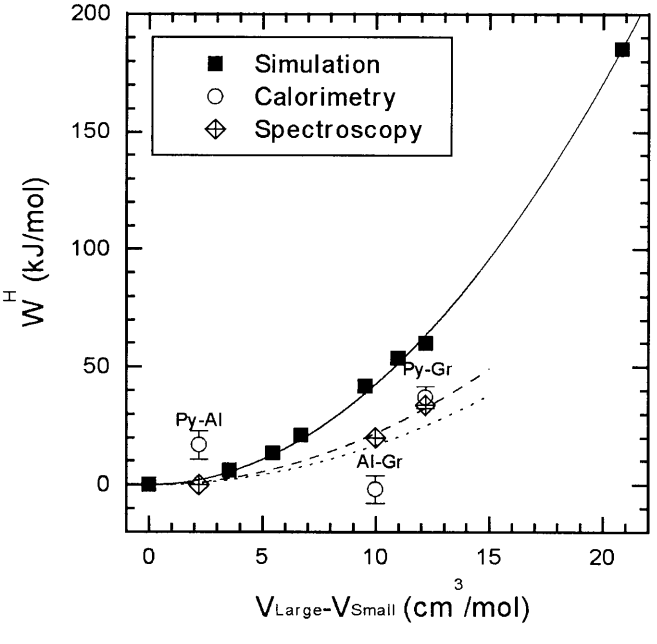

Fig. 6 Deviations from ideality for the enthalpies of mixing, quantified as W^H, as a function of the volume mismatch between end members. The simulated data from mixtures of Eka(n_{Mg}Mg/n_{Ca}Ca)-cations are shown as *full squares* and are fitted by a quadratic polynomial shown as a *full line*. Experimental data from calorimetry are shown as *open circles* and the *dotted curve* represents the best quadratic fit through the three data points, although there no obvious correlation with $V_{Large} - V_{Small}$. Experimental data from spectroscopic measurements (see explanation in text) on the same three garnet binaries are shown as *diamonds*, and the best fit through these data is shown as a *dashed line*. The sources of experimental data used are summarised in Table 1

Although the main purpose of the present study was to determine the role of ionic size on the magnitude of ΔV^{Mix}, we were curious to see whether a similar relationship also holds for ΔH^{Mix}. The enthalpies of mixing are thought to have two components: (1) a strain-energy term arising from the mismatch in size when one atom substitutes for the other and (2) a chemical energy term arising from the interactions of the atoms with their surroundings in the crystal lattice (e.g. Ganguly and Saxena 1987). Figure 6 shows the variation of W^H determined by simulating different Eka(Ca/Mg) solid solutions. As in the case of the volumes of mixing, W^H varies quadratically with ΔV_{AB}. Again, this dependency is entirely due to the size difference between the mixing cations. Hence, our simulations predict a quadratic scaling for the strain energy part of the enthalpies of mixing. Figure 6 also shows experimentally determined data for the symmetric Margules parameters of the enthalpies of mixing, W^H, as a function of $V_{Large}-V_{Small}$. Experimental data on enthalpies of mixing exist only for three of the six possible binary solid solutions, Py–Al, Al–Gr and Py–Gr. The symmetric Margules parameters, W^H, resulting from solution calorimetric measurements show no clear correlation with the volume mismatch between the end members (Fig. 6). Moreover, of the same three garnet binaries, Boffa Ballaran et al. (1999) studied the line-broadening of the IR active absorption bands as a function of garnet composition. Line-broadening is associated with local structural heterogeneities, which contribute to the excess elastic energy of a crystal. For Py–Gr and Al–Gr binaries, the effective line widths (Δ_{corr}) were found to vary in a non-linear way with composition, in a manner similar to the enthalpies of mixing. By empirically calibrating the observed broadening of the effective line widths with the enthalpies of solution of the Py–Gr binary, Boffa Ballaran et al. (1999) performed an analysis that allows a comparison of Δ_{corr} and ΔH^{Mix} on a quantitative scale. The calibrated data are suggested to give a direct measure of the strain-energy contribution to the enthalpies of mixing, $\Delta H^{Mix,strain}$. The corresponding $W^{H,strain}$ have been included in Fig. 6 and they scale quadratically with the volume mismatch, i.e. $W^{H,strain} \propto \Delta V_{AB}^2$. That this quadratic dependence is indeed predicted from our simulations for $\Delta H^{Mix,strain}$ supports the assumption of Boffa Ballaran et al. (1999) that the strain heterogeneity documented in their Δ_{corr} is a quantitative measure of elastic energy contributions to the enthalpies of mixing.

Conclusions

The simulations of the pyrope–grossular solid solutions using the supercell method are in sufficiently good agreement with experimental data that we can be confident that our model covers the main microscopic effects. By comparing simulations of pyrope–grossular solid solutions undertaken with two different levels of approximating solid solution, i.e. mixing potentials versus mixing cations in a supercell, it became apparent how significantly the macroscopic thermodynamic properties of garnet solid solutions are affected by local structural relaxations. In particular, allowing for local relaxations results in a decrease in the magnitude of the excess mixing properties, ΔV^{Mix} and ΔH^{Mix}, in comparison with the virtual crystal. Moreover, the variation of lattice constants, molar volumes and ΔV^{Mix} due to differences in ordering state could be deduced from simulations of pyrope–grossular solid solutions with the supercell method. From these, different X-site cation short-range ordering states are expected to result in variations in the lattice constants in the order of 0.002 Å.

Within any series of Eka(A/B)-solid solutions the mixing properties scale quadratically with the volume mismatch between the end members (Eq. 13). However, other changes in the magnitude of the mixing properties occur, which are due to other effects such as differences in the bonding character of the cations. Within a series of Eka(A/B)-solid solutions only the size difference between the mixing cations varies. Therefore, a quadratic dependency of the magnitude of the mixing properties on the volume mismatch is a result of local lattice strain due to the size mismatch between the cations being mixed. In fact, experimental data of ΔV^{Mix} and IR-spectroscopic data related to $\Delta H^{Mix,strain}$ both show a scaling with ΔV_{AB}^2, indicating that these properties are governed by lattice strain due to the cation size mismatch, and that other properties of the cations have only secondary influences.

Acknowledgements A. Bosenick acknowledges the award of a Marie Curie Fellowship by the European Community. M. Dove acknowledges support from NERC.

References

Ballaran TB, Carpenter MA, Geiger CA, Koziol AM (1999) Local structural heterogeneity in garnet solid solutions. Phys Chem Miner 26: 554–569

Berman RG (1990) Mixing properties of Ca–Mg–Fe–Mn garnets. Am Mineral 75: 328–344

Berman RG, Engi M, Greenwood HJ, Brown ThB (1986) Derivation of internally consistent thermodynamic data by the technique of mathematical programming: a review with application to the system MgO–SiO_2–H_2O. J Petrol 27: 1331–1364

Bosenick A, Geiger CA (1997) Powder diffraction study of synthetic pyrope-grossular garnets between 20 and 295 K. J Geophys Research 102: B10: 22649–22657

Bosenick A, Geiger CA, Schaller T, Sebald A (1995) An ^{29}Si MAS NMR and IR spectroscopic investigation of synthetic pyrope-grossular garnet solid solutions. Am Mineral 80: 691–704

Bosenick A, Geiger CA, Phillips BL (1999) Local Ca–Mg distribution of Mg-rich pyrope-grossular garnets synthesized at different temperatures revealed by ^{29}Si MAS NMR spectroscopy. Am Mineral 84: 1423–1433

Bosenick A, Dove MT, Geiger CA (2000) Simulation studies on the pyrope-grossular garnet solid solution. Phys Chem Miner 27: 398–418

Burnham CW (1985) Mineral structure energetics and modeling using the ionic approximation. Rev Miner 14: 347–388

Bush TS, Gale JD, Catlow CRA, Battle PD (1994) Self-consistent interatomic potentials for the simulation of binary and ternary oxides. J Mat Chem 4: 831–837

Catlow CRA (1988) Computer modeling of silicates. In: Salje EKH (ed) Physical properties and thermodynamic behaviour of minerals. NATO ASI series C, 225: 619–638, Reidel, Boston

Catlow CRA, Mackrodt WC (1982) Computer simulations of solids. Lecture notes in physics, vol 166, Springer, Berlin Heidelberg, New York

Catlow CRA, Mackrodt JR, Stewart RF (1982) Defect energies in aluminium oxide and rutile titanium oxide. Phys Rev (B)25: 1006–1026

Cemic L (1988) Thermodynamik in der Mineralogie. Springer, Berlin Heidelberg, New York

Chatterjee ND (1991) Applied mineralogical thermodynamics. Springer, Berlin Heidelberg, New York

Cormack AN (1999) Classical computer simulations. In: Wright K, Catlow CRA (eds) Microscopic properties and processes in minerals. NATO ASI series C, 543: 337–350, Kluwer Academic, Dordrecht

Davies PK, Navrotsky A (1983) Quantitative correlations of deviations from ideality in binary and pseudobinary solid solutions. J Solid State Chem 46: 1–22

Dove MT (1989) On the computer modeling of diopside: toward a transferable potential for silicate minerals. Am Mineral 74: 774–779

Dove MT (1993) Introduction to lattice dynamics. Cambridge University Press, Cambridge

Dove MT, Redfern SAT (1997) Lattice simulation studies of the ferroelastic phase transitions in $(Na,K)AlSi_3O_8$ and $(Sr,Ca)Al_2Si_2O_8$ feldspar solid solutions. Am Mineral 82: 8–15

Dove MT, Cool T, Palmer DC, Putnis A, Salje EKH, Winkler B (1993) On the role of Al–Si ordering in the cubic-tetragonal phase transition of leucite. Am Mineral 78: 486–492

Dove MT, Bosenick A, Myers ER, Warren MC, Redfern SAT (2000) Modelling in relation to cation ordering. Phase Transitions 71: 205–226

Gale JD (1997) GULP – a computer program for the symmetry adapted simulation of solids. JCS Faraday Trans 93: 629–637

Ganguly J, Kennedy GC (1974) The energetics of natural garnet solid solution. Contrib Miner Petrol 48: 137–148

Ganguly J, Saxena SK (1987) Mixtures and mineral reactions. Minerals and rocks, vol 19. Springer, Berlin Heidelberg New York

Ganguly J, Cheng W, O'Neill HStC (1993) Syntheses, volume, and structural changes of garnets in the pyrope–grossular join: implications for stability and mixing properties. Am Mineral 78: 583–593

Ganguly J, Cheng WJ, Tirone M (1996) Thermodynamics of aluminosilicate garnet solid solution: new experimental data, an optimized model, and thermometric applications. Contrib Mineral Petrol 126: 137–151

Geiger CA, Newton RC, Kleppa OJ (1987) Enthalpy of mixing of synthetic almandine–grossular and almandine–pyrope garnets from high-temperature solution calorimetry. Geochim Cosmochim Acta 51: 1755–1763

Geiger CA (1998) A powder infrared spectroscopic investigation of garnet binaries in the system $Mg_3Al_2Si_3O_{12}$–$Fe_3Al_2Si_3O_{12}$–$Mn_3Al_2Si_3O_{12}$–$Ca_3Al_2Si_3O_{12}$. E J Miner 10: 407–422

Geiger CA (1999) Thermodynamics of $(Fe^{2+}, Mn^{2+}, Mg, Ca)_3Al_2Si_3O_{12}$ garnet: a review and analysis. Miner Petrol 66: 271–299

Geiger CA (2000) Volumes of mixing in aluminosilicate garnets: implications for solid solution and strain behavior. Am Mineral 85: 893–897

Geiger CA, Rossmann GR (1994) Crystal field stabilization energies of almandine-pyrope and almandine-spessartine garnets determined by FTIR near infrared measurements. Phys Chem Miner 21: 516–525

Geiger CA, Feenstra A (1997) Molar volumes of mixing of almandine-pyrope and almandine-spessartine garnets and the crystal chemistry and thermodynamic-mixing properties of the aluminosilicate garnets. Am Mineral 82: 571–581

Hammonds KD, Bosenick A, Dove MT, Heine V (1998) Rigid unit modes in crystal structures with octahedrally coordinated atoms. Am Mineral 83: 476–479

Holland TJB, Powell R (1985) An internally consistent thermodynamic dataset with uncertainties and correlations: 1. Methods and a worked example. J Metamorph Geol, 3, 327–342

Koziol AM (1996) Quaternary (Ca–Fe–Mg–Mn) garnet: displaced equilibrium experiments and implications for current garnet mixing models. Eur J Miner 8: 453–460

Lewis GV (1984) Computer modelling of mixed oxides. PhD Thesis, University of London, University College

Mukhopadhyay B, Holdaway MJ, Koziol AM (1997) A statistical model of thermodynamic mixing properties of Ca–Mg–Fe^{2+} garnets. Am Mineral 82: 165–181

Navrotsky A (1987) Models of crystalline solid solutions. Rev Miner 17: 35–69

Newton RC, Charlu TV, Kleppa KM (1977) Thermochemistry of high pressure garnets and clinopyroxenes in the system CaO–MgO–Al_2O_3–SiO_2. Geochim Cosmochim Acta 41: 369–377

Olbricht W, Chatterjee ND, Miller K (1994) Bayes estimation – a novel approach to derivation of internally consistent thermodynamic data. Phys Chem Miner 21: 36–49

Patel A, Price GD, Mendelssohn MJ (1991) A computer simulation approach to modelling the structures, thermodynamics and oxygen isotope equilibria of silicates. Phys Chem Miner 17: 690–699

Payne MC, Teter MP, Allan DC, Arias TA, Joannopoulos JD (1992) Iterative minimization techniques for ab initio total energy calculations: molecular dynamics and conjugate gradients. Rev Mod Phys 64, 4: 1045–1097

Powell R, Holland TJB (1993) The applicability of least squares in the extraction of thermodynamic data from experimentally bracketed mineral equilibria. Am Mineral 78: 107–112

Price GD, Parker SC (1988) The computer simulation of the lattice dynamics of silicates. In: Salje EKH (ed) Physical properties and thermodynamic behaviour of minerals. NATO ASI Series C, 225: 591–618, Riedel, Boston

Price GD, Parker SC, Leslie M (1987) The lattice dynamics and thermodynamcis of the Mg_2SiO_4 polymorphs. Phys Chem Miner 15: 181–190

Purton JA, Blundy JD, Taylor MB, Barrera GD, Allan NL (1998) Hybrid Monte Carlo and lattice dynamics simulations: the enthalpy of mixing of binary oxides. J Chem Soc, Chem Commun, pp 627–628

Quartieri S, Chaboy J, Merli M, Oberti R, Ungaretti L (1995) Local structural environment of calcium in garnets – a combined structure refinement and XANES investigation. Phys Chem Miner 22: 159–169

Redfern SAT, Dove MT, Wood DRR (1997) Static lattice simulation of feldspar solid solutions: ferroelastic instabilities and order/disorder. Phase Trans 61: 173–194

Sanders MJ, Leslie M, Catlow CRA (1984) Interatomic potentials for SiO_2. J Chem Soc, Chem Commun 19: 1271–1273

Thompson JB (1969) Chemical reactions in crystals. Am Mineral 54: 341–375

Ungaretti L, Leona M, Merli M, Oberta R (1995) Non-ideal solid-solution in garnet: crystal-structure evidence and modelling. Eur J Miner 7: 1301–1312

Warren MC, Dove MT, Redfern SAT (2000) Ab initio simulations of cation ordering in oxides: application to spinel. J Phys Condense Matt 12: L43–L48

Winkler B, Dove MT, Leslie M (1991) Static lattice energy minimization and lattice dynamics calculations on aluminosilicate minerals. Am Mineral 76: 313–331